



## Long-term field measurement and analysis of the natural wind characteristics at the site of Xi-hou-men Bridge<sup>\*</sup>

Ming LIU<sup>†1</sup>, Hai-li LIAO<sup>1</sup>, Ming-shui LI<sup>1</sup>, Cun-ming MA<sup>1</sup>, Mei YU<sup>1,2</sup>

(<sup>1</sup>Research Center for Wind Engineering, Southwest Jiaotong University, Chengdu 610031, China)

(<sup>2</sup>Chongqing Jiaotong University, Chongqing 400074, China)

<sup>†</sup>E-mail: lium\_03@163.com; rainmanok@gmail.com

Received July 5, 2011; Revision accepted Dec. 7, 2011; Crosschecked Feb. 13, 2012

**Abstract:** In order to investigate the wind characteristics of coastal areas of China, a long-term field measurement of natural wind was carried out. Based on the field measurement results, this paper presents the natural wind characteristics of typhoons and strong monsoons at the site of Xi-hou-men Bridge, including mean wind speed, mean wind direction, mean wind elevation angle, turbulent intensity, gust factor, turbulence integral length scales, power spectrum of wind speed and spatial correlation of gusty wind, the profiles of mean wind speed and turbulent intensity, etc. The correlation among wind characteristics is analyzed in detail, and the similarities and differences of wind characteristics between typhoons and monsoons are analyzed. These results can provide detailed wind characteristics of coastal areas of China.

**Key words:** Wind characteristics, Field measurement, Wind spectrum, Wind profiles, Spatial correlation  
**doi:**10.1631/jzus.A1100178 **Document code:** A **CLC number:** U44

### 1 Introduction

Field measurement of wind characteristics is one of the basic research areas on bridge wind engineering. The wind characteristics results based on field measurement can provide a reference for the modification of wind tunnel testing and simulation technology. Long-span suspension bridges are susceptible to wind excitation due to relatively small mass and extremely low inherent damping. The effect of wind-induced response has to be taken into account in the design and construction.

Xi-hou-men Bridge, located in the Xi-hou-men Bay of Zhoushan City of China, is one of the longest span suspension bridges. It has a total length of 2713 m, a main span of 1650 m, and two side spans of

578 and 485 m, respectively. The girder is 36 m wide with four traffic lanes, with a clearance height approximately 72 m above water level. Xi-hou-men Bay is one of the regions most badly impacted by typhoons and strong monsoons in the world. Hence, the bridge is subjected to fierce wind forces induced by typhoons and strong monsoons. All these facts make a detailed study of wind effects on the long span bridge important and necessary. To investigate wind characteristics and to provide reliable field measurement data for the design and construction, four ultrasonic anemometers were installed on the bridge deck, 3.5 m above the deck and about 75.5 m above the sea surface. Eleven propeller anemometers were installed near bridge tower to measure the profiles of mean wind speed and turbulence intensity. Three receivers of global positioning system (GPS) were installed on the bridge deck. The layout of anemometers and GPS are shown in Fig. 1. The installation station of field measurement apparatus is shown in Figs. 2 and 3. The 81000 ultrasonic anemometer

<sup>\*</sup> Project supported by the National Natural Science Foundation of China (No. 50808148), and the National Key Technology R&D Program (No. 2008BAG07B02), China  
 © Zhejiang University and Springer-Verlag Berlin Heidelberg 2012

produced by R.M. Yong Company is adopted for the turbulence wind characteristics in which wind speed ranges from 0 to 40 m/s, azimuth ranges from  $0.0^\circ$  to  $359.9^\circ$  and elevation ranges from  $-60^\circ$  to  $60^\circ$ . The 05103V propeller anemometer produced by R.M. Yong Company is adopted for the profiles of mean wind speed and turbulent intensity in which wind speed ranges from 0 to 100 m/s, and azimuth ranges from  $0.0^\circ$  to  $359.9^\circ$ . In the field measurement, the sampling frequency was set to 100 Hz. The field measurement at this bridge was conducted from Oct., 2007 to Mar., 2009. This paper is based on the field measurement of typhoon “Rosa” and some extremely strong monsoons.

## 2 Modification of field data

As the duration time of field measurement is very long, enormous field data are obtained. Many field data of low wind speed are included only for the continuity of field data. But the field data of low wind speed are insignificant for the wind characteristics. So a “Strong Wind Principle” is adopted, which means that the field data of mean speed greater than 8 m/s are applied in the analysis of wind characteristics and others are eliminated (Pang, 2006).

In addition, to reflect the real wind characteristics of mid-span of Xi-hou-men Bridge, the measured position is set in the mid-span on the deck. Due to the limitation of installation position, four ultrasonic anemometers are 3.5 m above the deck which may

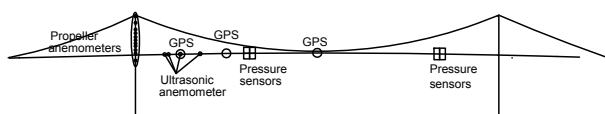


Fig. 1 Layout of sensors of wind speed, wind pressure and buffeting response



Fig. 2 Locations of 81000 ultrasonic anemometers

influence the results of wind characteristics. So a computational fluid dynamics (CFD) simulation method is used to modify the influence of deck height to the field measurement data. Fig. 4 shows the local computational domain and grid around the deck. These boundaries are sufficiently far away from the cross-section. Using the CFD method, the wind speed is obtained at the observation position assuming the incoming flow wind speed ranges from 0–50 m/s. Vector-graph of wind speed is shown in Fig. 5 in which the inlet wind speed is 15 m/s and the attack angle is  $-4^\circ$ . Similarly, wind elevation angle is

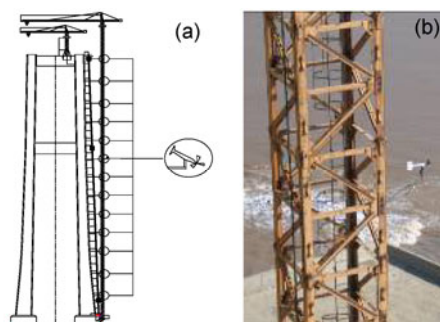


Fig. 3 Locations of anemometers for mean wind speed profiles (a); Photo of 05103V propeller anemometer (b)

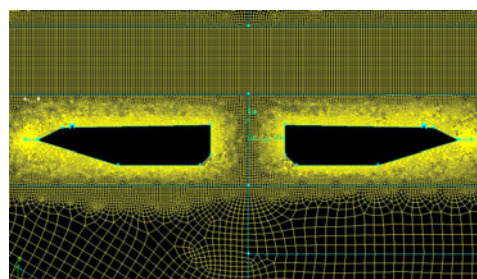


Fig. 4 Local computational domain and grid around deck

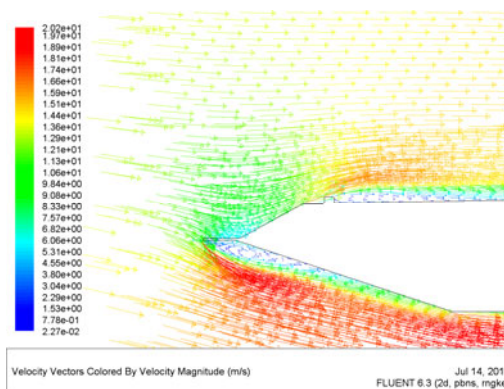


Fig. 5 Vector-graph of wind speed (inlet speed 15 m/s, attack angle  $-4^\circ$ )

obtained assuming the incoming flow wind elevation angle ranges from  $-10^\circ$  to  $10^\circ$ . The correlation relationship of wind speed and wind elevation angle between observation position and incoming flow can be expressed by Eq. (1). The wind speed and wind azimuth around bridge tower can be modified by the same method.

The modified expression of wind elevation angle is

$$y=0.00502x^2+0.54235x-2.6855, -10^\circ \leq x \leq 0^\circ, \quad (1a)$$

$$y=0.01312x^2+0.31132x-1.58705, 0^\circ < x \leq 10^\circ; \quad (1b)$$

and the modified expression of wind speed is

$$y=0.0063x^2+0.2644x+0.90971, \quad (1c)$$

where  $y$  is the wind elevation angle or wind speed of incoming flow, and  $x$  is the wind elevation angle or wind speed at observation position.

### 3 Wind characteristics of boundary layer wind

#### 3.1 Turbulence intensity and gust factor

Turbulence intensity and gust factor are two important parameters to describe the wind characteristics of boundary layer fluctuating wind speed, and are also useful to determine design wind loads on structure. Turbulence intensity is defined as the ratio of the standard deviation of the speed component to the longitudinal mean wind speed in a certain duration (normally 10 min), respectively. It can be described as (Li *et al.*, 2007; Fu *et al.*, 2008)

$$I_i = \frac{\sigma_i}{U}, \quad (2)$$

where  $\sigma_i$  ( $i=u, v, w$ ) is the standard deviation of the speed component, and  $U$  is the mean wind speed.

Gust factor is defined as the ratio of the max gust speed within gust duration  $t_g$  to the mean wind speed  $U$  in a certain duration (Li *et al.*, 2007):

$$G_u(t_g) = 1 + \frac{\max(u(t_g))}{U}, \quad (3a)$$

$$G_v(t_g) = \frac{\max(v(t_g))}{U}, \quad (3b)$$

$$G_w(t_g) = \frac{\max(w(t_g))}{U}, \quad (3c)$$

where  $t_g$  is adopted as 3 s in this study, and  $G_u, G_v, G_w$  is the longitudinal, lateral, and vertical gust factor, respectively,  $u, v$ , and  $w$  is the longitudinal, lateral and vertical turbulence wind speed, respectively. Normally, the gust factor decreases with the increase of gust duration  $t_g$ , and the longitudinal gust factor  $G_u$  decreases to 1 when the gust duration  $t_g$  is 10 min.

#### 3.2 Friction velocity

Friction velocity indicates the vertical energy loss of horizontal average momentum because of ground roughness. It can be calculated by (Li *et al.*, 2008)

$$u_*^2 = -\overline{uw} - \overline{vw}, \quad (4)$$

where  $u_*$  is the friction velocity, and a bar means the average value.

To eliminate the effect of instability of atmosphere, the following expression is adopted to eliminate the effect of instability (Tieleman, 1983; Li *et al.*, 2008):

$$u_*^2 = \sqrt{(\overline{uw})^2 + (\overline{vw})^2}. \quad (5)$$

Eq. (5) can eliminate the probability of the Reynolds stress that is negative value. Therefore, Eq. (5) is adopted in this study.

#### 3.3 Turbulence integral length scale

Turbulence integral length scale is another important parameter for describing the turbulence characteristics. The turbulence length scales define the position of the turbulence spectral content (Solari and Piccardo, 2001). It is often interpreted as the wavelength corresponding to the maximum normalized spectral density. The turbulence integral length scale can be estimated by fitting the field measured spectrum to the theoretic spectrum. Relative to other estimated methods, this method has the advantage of fitting the whole spectrum rather than only the

position of the peak. The von Karman spectrum Eq. (6) are usually used as the theoretic spectrum (Solari and Piccardo, 2001; Fu et al., 2008; Hui et al., 2009a; 2009b).

$$\frac{nS_u(n)}{\sigma_u^2} = \frac{4L_u n / U}{[1 + 70.8(L_u n / U)^2]^{5/6}}, \quad (6a)$$

$$\frac{nS_v(n)}{\sigma_v^2} = \frac{(4L_v n / U)[1 + 755.2(L_v n / U)^2]}{[1 + 283.2(L_v n / U)^2]^{11/6}}, \quad (6b)$$

$$\frac{nS_w(n)}{\sigma_w^2} = \frac{(4L_w n / U)[1 + 755.2(L_w n / U)^2]}{[1 + 283.2(L_w n / U)^2]^{11/6}}, \quad (6c)$$

where  $n$  is the frequency of natural wind,  $L_u$ ,  $L_v$ ,  $L_w$  is turbulence integral length scale of longitudinal, lateral and vertical, respectively,  $S_u$ ,  $S_v$ ,  $S_w$  is the wind speed spectrum of longitudinal, lateral and vertical, respectively.

### 3.4 Power spectrum of wind speed

Power spectrum of wind speed describes the energy distribution of fluctuating wind velocity in the frequency domain, which presents descriptions of frequency characteristics of fluctuating wind speed. The power spectrum of every sub-sample was calculated using the Fast Fourier Transform technique (FFT) on transforming the fluctuating wind velocity from time domain to frequency domain. The field measurement power spectrum is obtained by averaging the power spectrum of all sub-samples. As the Kaimal spectrum and Panofsky spectrum have been recommended by Wind-Resistant Design Specification of China, the following experiential expressions are adopted:

Longitudinal wind spectrum:

$$\frac{nS_u(n)}{\sigma_u^2} = \frac{A_u f}{(1 + B_u f)^{5/3}}, \quad (7a)$$

Lateral wind spectrum:

$$\frac{nS_v(n)}{\sigma_v^2} = \frac{A_v f}{(1 + B_v f)^{5/3}}, \quad (7b)$$

Vertical wind spectrum:

$$\frac{nS_w(n)}{\sigma_w^2} = \frac{A_w f}{(1 + B_w f)^2}, \quad (7c)$$

where  $f$  is the non-dimension frequency,  $f=nz/U$ ,  $z$  is the height.  $A_u$ ,  $B_u$ ,  $A_v$ ,  $B_v$ ,  $A_w$ ,  $B_w$  are parameters.

## 4 Results of wind characteristics

### 4.1 Field results of typhoon "Rosa"

#### 4.1.1 Mean wind speed and mean direction of Typhoon "Rosa"

Typhoon "Rosa" attacked Xi-hou-men Bridge from Oct. 6 to 7, 2007. A total of 31 h field measurement data were recorded. The whole typhoon measured data were divided into 186 sub-samples of 10-min duration. Fig. 6 shows the variations of 10-min mean wind speed, 10-min mean wind elevation angle and 10-min mean wind direction of typhoon. It was found that the maximum 10-min mean wind speed was 15.9 m/s. During the duration of the typhoon, the mean elevation angle was of negative value, which ranged from  $-0.85^\circ$  to  $-4.0^\circ$ , and the mean value of wind elevation angle was  $-2.25^\circ$ .

#### 4.1.2 Turbulence intensity and gust factor of typhoon "Rosa"

According to Eqs. (2) and (3), the longitudinal turbulence intensity ( $I_u$ ) of typhoon "Rosa" ranged from 0.08 to 0.29, the lateral turbulence intensity ( $I_v$ ) ranged from 0.06 to 0.20, and the vertical turbulence intensity ( $I_w$ ) ranged from 0.01 to 0.09. The mean values of  $I_u$ ,  $I_v$  and  $I_w$  were 0.17, 0.11 and 0.04, respectively. The ratio amongst them was  $I_u:I_v:I_w=1:0.67:0.24$ . The mean values of  $G_u$ ,  $G_v$  and  $G_w$  were 1.38, 0.28, and 0.11, respectively. The turbulence intensity and gust factor were greater than the recommended value of Wind-Resistant Design Specification of China. Figs. 7 and 8 show the distributions of turbulence intensities and gust factors of typhoon "Rosa". It can be seen that the distributions of turbulence intensities and gust factors are random, indicating the randomness of typhoon.

Fig. 9 presents the relationship between turbulence intensities of typhoon "Rosa". It can be seen that there is a linear relationship between the turbulence intensities. Fig. 10 presents the relationship

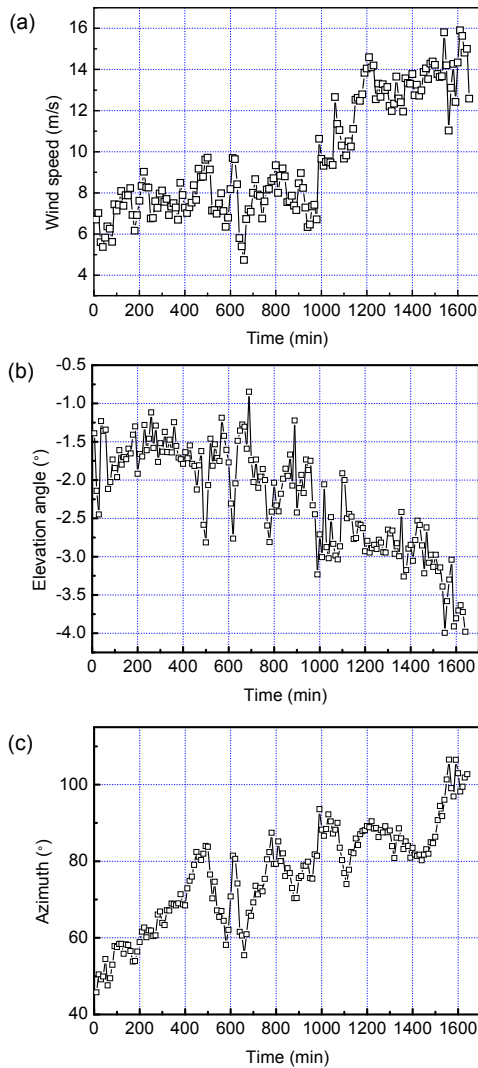


**Fig. 6** Variations of typhoon “Rosa” of (a) 10-min mean wind speed; (b) 10-min mean wind elevation angle; and (c) 10-min mean wind azimuth

between the turbulence intensities in longitudinal, lateral and vertical directions to the mean wind speed. It can be seen that there are tendencies for the turbulence intensities to decrease with the increase of mean wind speed. Fig. 11 presents the relationship between the longitudinal turbulence intensities and longitudinal gust factor. It can be seen that there is a linear relationship between the turbulence intensities and gust factors, and can be expressed as  $G_u=1+2.3I_u$ .

#### 4.1.3 Friction velocity of Typhoon “Rosa”

Fig. 12 shows the relationship between the friction velocity and mean wind speed. It can be found that the square value of friction velocity increases

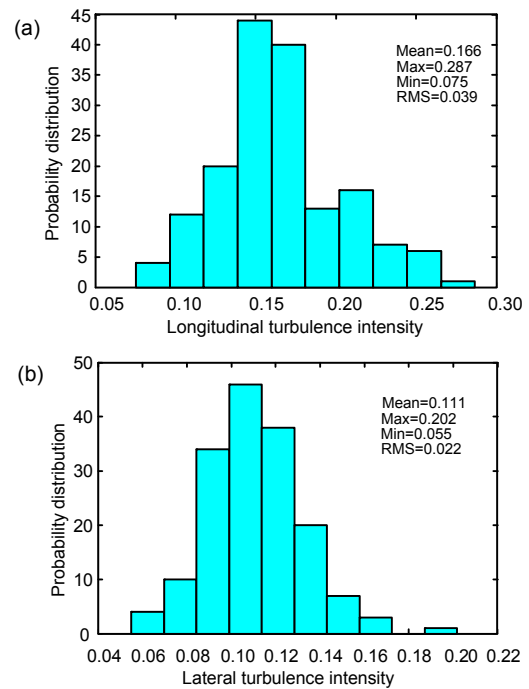


**Fig. 7** Distribution of turbulence intensity (a) Longitudinal; (b) Lateral

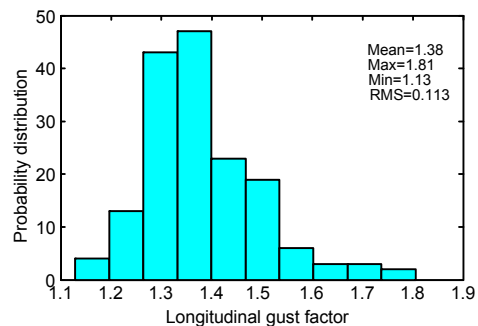


**Fig. 8** Distribution of longitudinal gust factor

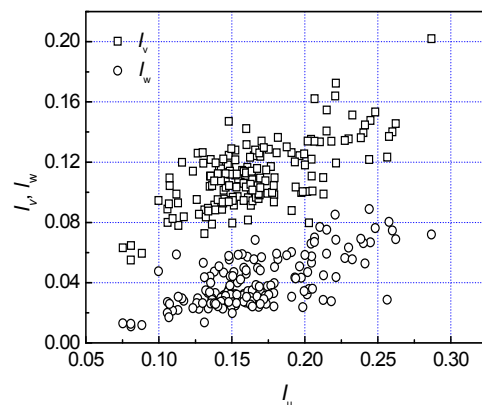


**Fig. 9** Relationship between turbulence intensities of typhoon “Rosa”

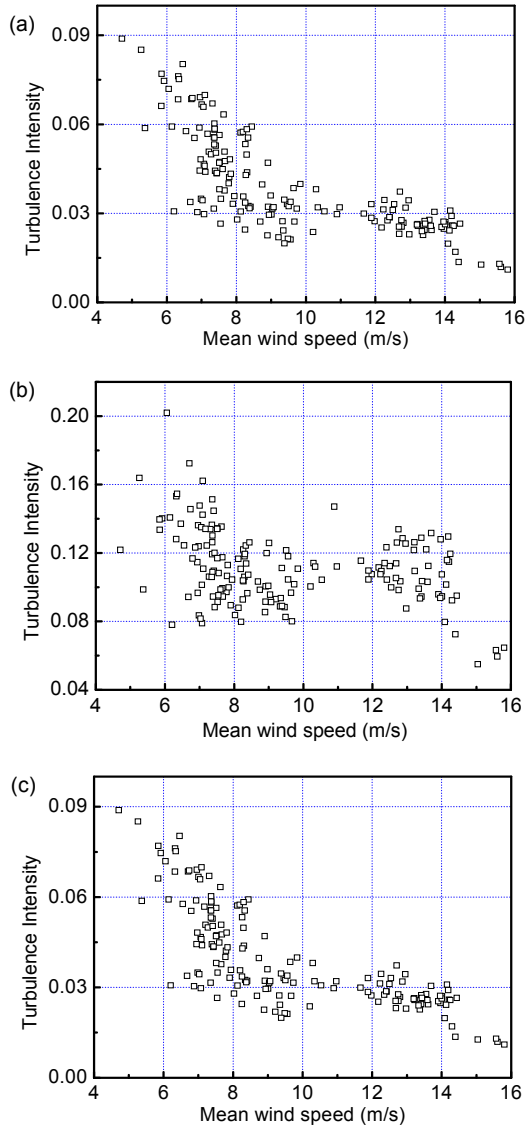


**Fig. 10 Relationship between the turbulence intensity and mean wind speed**  
 (a) Longitudinal; (b) Lateral; (c) Vertical

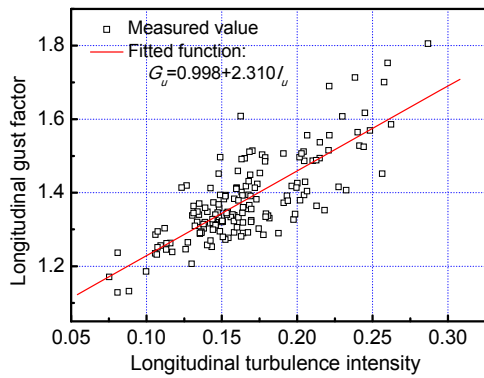


**Fig. 11 Relationship between the longitudinal turbulence intensity and longitudinal gust factor**

with the increase of mean wind speed. The relationship between the friction velocity  $u_*$  and longitudinal standard deviation  $\sigma_u$  is shown in Fig. 13 and can be described as

$$\sigma_u^2 = -0.43 + 3.59u_*^2. \quad (8)$$

4.1.4 Turbulence integral length scale of Typhoon “Rosa”

Fig. 14 shows the distribution of integral length scales of Rosa. The mean values of longitudinal

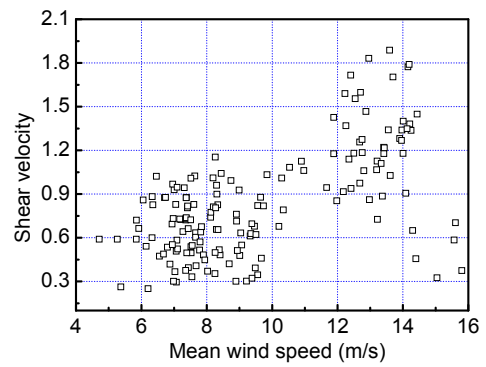


**Fig. 12 Relationship between the mean wind speed and shear velocity ( $u_*^2$ )**

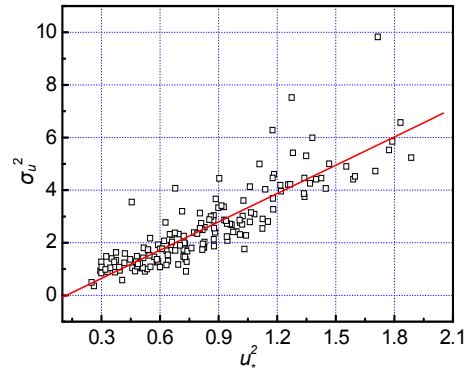


**Fig. 13 Relationship between friction velocity  $u_*$  and standard deviation  $\sigma_u$**

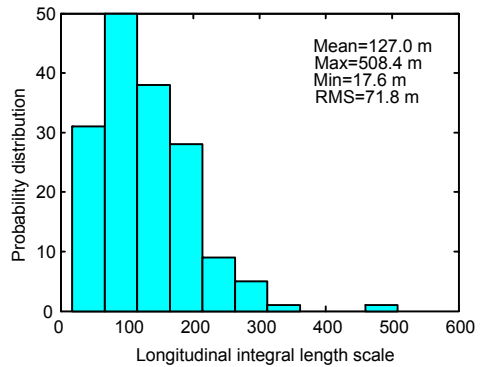


**Fig. 14 Distribution of longitudinal integral length scales**

integral length scale ( $L_u$ ), lateral integral length scale ( $L_v$ ) and vertical integral length scale ( $L_w$ ) were 127, 73, and 23 m, respectively. The ratio among them was  $L_u:L_v:L_w=1:0.58:0.18$ .

Fig. 15 presents the relationship between the turbulence integral length scales and mean wind speed. It can be seen that there are tendencies for the turbulence integral length scales to increase with the increase of the mean wind speed.

4.1.5 Power spectrum of typhoon “Rosa”

Fig. 16 shows the normalized power spectrum of longitudinal, lateral and vertical of typhoon “Rosa”. Fitting the field measured spectrum to the theoretic spectrum Eq. (7), the following expressions can be obtained to describe the normalized power spectrum of typhoon “Rosa” at the site of Xi-hou-men Bridge.

Longitudinal wind spectrum:

$$\frac{nS_u(n)}{\sigma_u^2} = \frac{3.84f}{(1+6.89f)^{5/3}}; \tag{9a}$$

Lateral wind spectrum:

$$\frac{nS_v(n)}{\sigma_v^2} = \frac{2.41f}{(1+3.93f)^{5/3}}; \tag{9b}$$

Vertical wind spectrum:

$$\frac{nS_w(n)}{\sigma_w^2} = \frac{0.19f}{(1+0.15f)^2}. \tag{9c}$$

4.2 Field results of strong monsoons

4.2.1 Turbulence intensity and turbulence integral length scale

Fig. 17 shows the distribution of turbulence intensities and gust factors of strong monsoons. The mean values of longitudinal, lateral and vertical turbulence intensities were  $I_u=0.105$ ,  $I_v=0.093$ , and  $I_w=0.063$ , respectively, and the ratio of them was  $I_u:I_v:I_w=1:0.87:0.58$ , which is similar to the recommended value of Wind-Resistant Design Specification for Highway Bridges of China.

Fig. 18 shows the distribution of integral length scales of strong monsoons. The mean values of

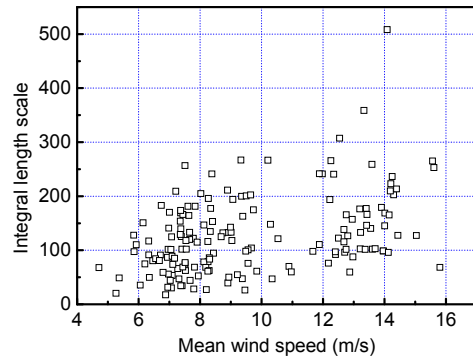


Fig. 15 Relationship between the longitudinal integral length scales and 10-min mean wind speed of typhoon “Rosa”

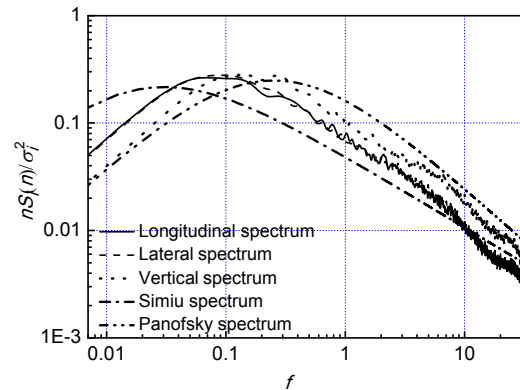


Fig. 16 Power spectrum density of wind speed of typhoon “Rosa”

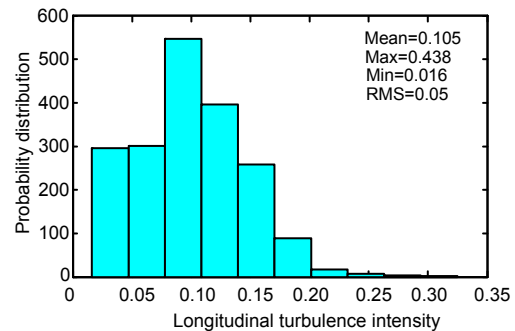


Fig. 17 Distribution of longitudinal turbulence intensity

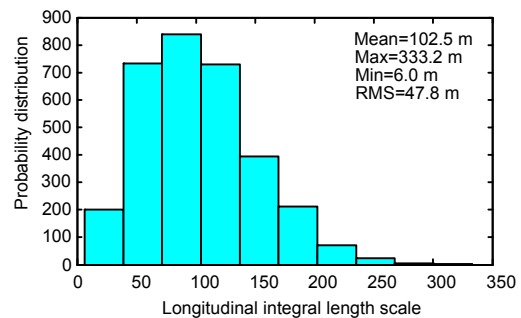


Fig. 18 Distribution of longitudinal integral length scales

longitudinal integral length scale ( $L_u$ ), lateral integral length scale ( $L_v$ ) and vertical integral length scale ( $L_w$ ) were 102.5, 44.2, and 15.4 m, respectively. The ratio among them was  $L_u:L_v:L_w=1:0.43:0.15$ .

4.2.2 Friction velocity and power spectral density of strong monsoon

At the strong monsoons, the relationship between the friction velocity  $u_*$  and standard deviation  $\sigma_u$  can be described as

$$\sigma_u^2 = 0.05 + 1.26u_*^2. \tag{10}$$

Fig. 19 shows the envelope curve of power spectral density of wind speed in strong monsoons. The power spectral density of strong monsoons can be described as

Longitudinal wind spectrum:

$$\frac{nS_u(n)}{\sigma_u^2} = \frac{23.41f}{(1 + 30.63f)^{5/3}}; \tag{11a}$$

Lateral wind spectrum:

$$\frac{nS_v(n)}{\sigma_v^2} = \frac{20.92f}{(1 + 29.31f)^{5/3}}; \tag{11b}$$

Vertical wind spectrum:

$$\frac{nS_w(n)}{\sigma_w^2} = \frac{5.24f}{(1 + 5.51f)^2}. \tag{11c}$$

4.2.3 Mean wind profiles and turbulence intensity profiles

Mean wind speed profile is defined to describe the changing of mean wind speed with the change of height. At present, the mean wind speed profile can be expressed by power law or logarithmic law. The power law has been adopted by the Wind-Resistant Design Specification of China. Therefore, this study adopts the power law. It is expressed as Eq. (12) (Dai et al., 2009). Because of the randomness of turbulence, the results are very discrete. To compare various results, the field measured results in each height are normalized. The profiles of mean wind speed and longitudinal turbulence intensity are shown in Fig. 20 and Fig. 21, respectively. It can be seen that they

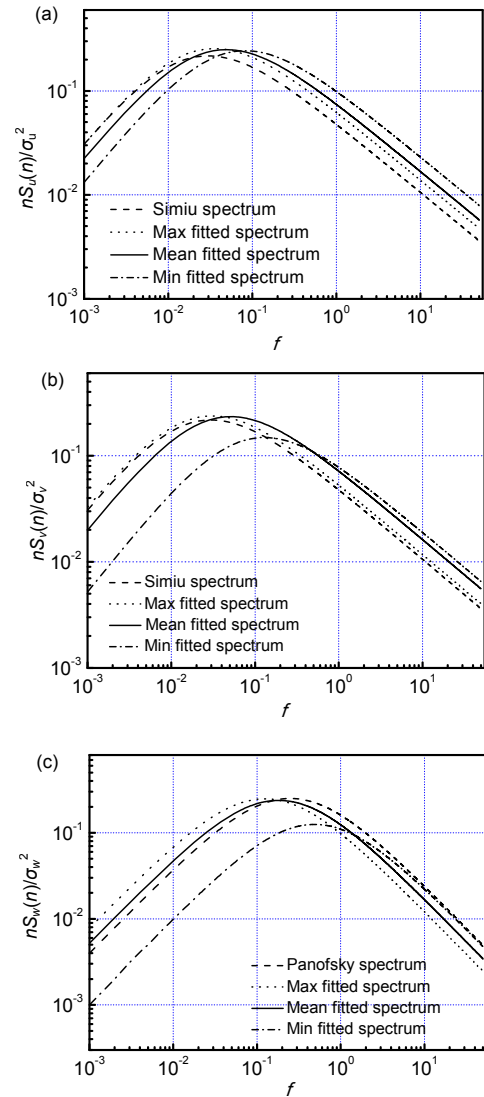


Fig. 19 Envelope curve of power spectral density during strong monsoon (a) Longitudinal; (b) Lateral; (c) Vertical

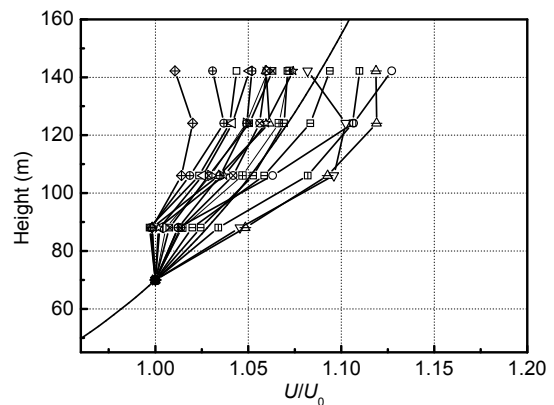


Fig. 20 Profiles of mean wind speed

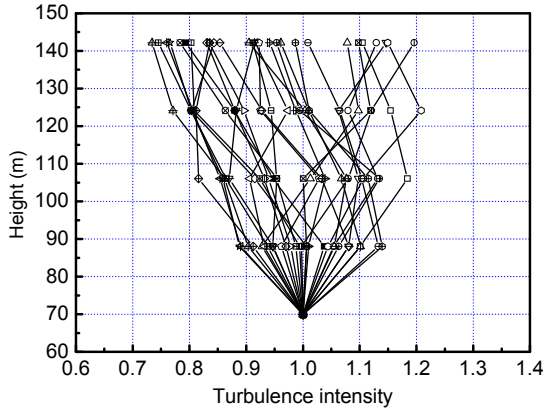


Fig. 21 Profiles of turbulence intensity

do not comply to the power law strictly. The reason may be (1) the randomness of atmosphere system; (2) the atmosphere has strong vortex movement and strong vertical hybrid movement which accede to the influence of rough condition seriously; (3) the wind field is disturbed by the terrain nearby.

$$\frac{U}{U_0} = \left(\frac{z}{z_0}\right)^\alpha, \tag{12a}$$

$$\frac{I_u}{I_{u0}} = \left(\frac{z}{z_0}\right)^\beta, \tag{12b}$$

where  $U$  and  $U_0$  is the mean wind speed at height  $z$  and  $z_0$ , respectively.  $I_u$  and  $I_{u0}$  is the turbulent intensity at height  $z$  and  $z_0$ , respectively.  $\alpha$  is the mean wind profile exponent, and  $\beta$  is the turbulent intensity exponent.

Table 1 presents some mean wind profile exponents. The range of variation is quite large, the maximum value can be up to 0.12 and the minimum value can be as small as 0.064, or even a negative value (it means that the profile of mean wind cannot obey the power law). The mean value of wind speed profile exponent  $\alpha$  is 0.097. As shown in Table 1, the exponent  $\alpha$  is directional. In the same wind direction, there is a tendency for the exponent  $\alpha$  to decrease with the increase of mean wind speed. Table 2 presents the exponents of turbulence intensity profile. It can be seen that the rule of turbulence intensity profile is similar to the mean wind profile.

#### 4.2.4 Spatial correlation of winds

At present, there are very few field measurement results about spatial correlation of natural wind. In the

wind-resistant design, the decay factor is often set to be 7, which affects the wind-resistant design of long span bridge. Therefore, the spatial correlation of winds at the site of Xi-hou-men Bridge is very important and necessary.

To determine the spatial correlation of wind, co-coherence of wind records are calculated, which is defined as (Toriumi *et al.*, 2000; Solari and Piccardo, 2001; Miyata *et al.*, 2002; Hui *et al.*, 2009b)

$$\begin{aligned} \text{Co-coherence} &= \frac{S_{uu}^C(x_1, x_2, f)}{\sqrt{S_{uu}(x_1, f)S_{uu}(x_2, f)}} \\ &= \exp\left(-k \frac{f \Delta y}{U}\right), \end{aligned} \tag{13}$$

where  $S_{uu}(x_1, f)$ ,  $S_{uu}(x_2, f)$  is the spectrum of wind speed fluctuation  $u$  at  $x_1$  and  $x_2$ , respectively.  $S_{uu}^C(x_1, x_2, f)$  is the real part of cross-spectrum of  $u$  between  $x_1$  and  $x_2$ ,  $k$  is the decay factor, and  $\Delta y = |x_1 - x_2|$  is the transverse distance.

The field measurement results of decay factors are shown in Table 3. The transverse distance is 18 m. It can be seen that the decay factors range widely. The decay factor for the along wind  $C_{uu}$  ranges from 8.7 to 22.7, the factor for crosswind  $C_{vv}$  ranges from 7.8 to 13.2, and the factor for vertical components  $C_{ww}$  ranges from 13.4 to 23.4. The average values are  $C_{uu}=16.7$ ,  $C_{vv}=10.1$ , and  $C_{ww}=18.8$ , respectively. The

Table 1 Wind profiles exponents at the site of Xi-hou-men Bridge

Date	$\alpha$	Mean speed (m/s)	Azimuth
Mar. 17, 2009	0.120	9.02	SSE
Mar. 21, 2009	0.064	11.17	SE
Mar. 26, 2009	0.084	10.00	SE
Mar. 27, 2009	0.111	8.52	ESE
Apr. 19, 2009	0.107	12.41	SSE

S: south; E: east

Table 2 Turbulence intensity profiles exponents at the site of Xi-hou-men Bridge

Date	$\beta$	Mean speed (m/s)	Azimuth
Mar. 17, 2009	-0.159	9.02	SSE
Mar. 21, 2009	-0.089	11.17	SE
Mar. 26, 2009	-0.076	10.00	SE
Mar. 27, 2009	-0.053	8.52	ESE
Apr. 19, 2009	0.032	12.41	SSE

S: south; E: east

**Table 3** Decay factors at the site of Xi-hou-men Bridge

Date	$C_{uu}$	$C_{vv}$	$C_{ww}$	$U$ (m/s)
Nov. 8, 2008	21.5	10.9	21.6	12.06
Nov. 19, 2008	17.6	9.0	23.2	10.93
Nov. 27, 2008	22.7	11.7	22.9	14.68
Dec. 1, 2008	20.3	10.7	21.0	12.19
Dec. 4, 2008	22.7	13.2	23.4	14.91
Dec. 5, 2008	21.2	12.8	20.7	14.46
Mar. 17, 2009	11.9	7.8	15.0	8.99
Mar. 21, 2009	12.6	8.6	17.2	11.21
Mar. 26, 2009	8.7	9.8	13.4	9.99
Mar. 27, 2009	14.8	8.8	14.7	8.51
Apr. 18, 2009	12.5	8.6	15.8	10.05
Apr. 19, 2009	13.8	9.3	17.0	12.23
Average value	16.7	10.1	18.8	11.60

recommended value of Wind-Resistant Design Specification for Highway Bridges of China is  $C=7-21$ , and  $C=7$  is applied in the design of long-span bridge, which is too conservative to be economic. The field measurement results within the recommended value, and are similar to the field results of Pang (2006) at the site of Sutong Bridge which are  $C_{uu}=16.2$ ,  $C_{vv}=15.0$ , and  $C_{ww}=17.0$ , respectively. The field measurement value of Akashi-Kaikyo Bridge ranges from 4 to 17, and the average value of all data is 9.3 (Toriumi *et al.*, 2000). The field measurement results at the site of Xi-hou-men Bridge show that the winds are less coherent in comparison with that assumed in the design, and the lateral component is more coherent than longitudinal component and vertical component.

## 5 Conclusions

This paper presents part results of the field measurements at the site of Xi-hou-men Bridge. Wind characteristics and the relationships among them are analyzed and discussed in detail. Some conclusions from this study are summarized as follows.

1. At typhoon "Rosa", the mean values of turbulence intensities  $I_u$ ,  $I_v$  and  $I_w$  are 0.17, 0.11 and 0.04, respectively, and the ratio among them is  $I_u:I_v:I_w=1:0.67:0.24$ . The mean values of  $L_u$ ,  $L_v$  and  $L_w$  are 127, 73 and 23 m and the ratio amongst them is  $L_u:L_v:L_w=1:0.58:0.18$ . At strong monsoons, the mean values of turbulence intensities  $I_u$ ,  $I_v$  and  $I_w$  are 0.105,

0.093 and 0.063, respectively and the ratio among them is  $I_u:I_v:I_w=1:0.87:0.58$ , which is similar to the recommended value of Wind Resistant Design Specification for Highway Bridges of China. The mean values of  $L_u$ ,  $L_v$  and  $L_w$  are 102.5, 44.2 and 15.4 m and the ratio among them is  $L_u:L_v:L_w=1:0.43:0.15$ . It can be seen that the wind characteristics of typhoons and monsoons are quite different. The turbulence intensities of typhoons are greater than those of monsoons and the recommended value. The turbulence integral length scales of typhoons are greater than those of monsoons. This means the atmosphere of typhoons is more complex than that of monsoons.

2. From the relationship between wind characteristics, it can be found that the turbulence intensities decrease with the increase of mean wind speed, and the turbulence integral length scales increase with the increase of mean wind speed.

3. At typhoon "Rosa", the relationship between the friction velocity  $u_*$  and standard deviation  $\sigma_u$  can be described as

$$\sigma_u^2 = -0.43 + 3.59u_*^2.$$

At the strong monsoons, the relationship is

$$\sigma_u^2 = 0.05 + 1.26u_*^2.$$

4. At typhoon "Rosa", the power spectral density of wind can be described as

Longitudinal wind spectrum:

$$\frac{nS_u(n)}{\sigma_u^2} = \frac{3.84f}{(1 + 6.89f)^{5/3}};$$

Lateral wind spectrum:

$$\frac{nS_v(n)}{\sigma_v^2} = \frac{2.41f}{(1 + 3.93f)^{5/3}};$$

Vertical wind spectrum:

$$\frac{nS_w(n)}{\sigma_w^2} = \frac{0.19f}{(1 + 0.15f)^2}.$$

At strong monsoons the expressions can describe

as follows:

Longitudinal wind spectrum:

$$\frac{nS_u(n)}{\sigma_u^2} = \frac{23.41f}{(1 + 30.63f)^{5/3}};$$

Lateral wind spectrum:

$$\frac{nS_v(n)}{\sigma_v^2} = \frac{20.92f}{(1 + 29.21f)^{5/3}};$$

Vertical wind spectrum:

$$\frac{nS_w(n)}{\sigma_w^2} = \frac{5.24f}{(1 + 5.51f)^2}.$$

5. The field measured results show that the range of mean wind profiles is quite wide, the maximum value can up to 0.12 and the minimum value can be as small as 0.064, or even a negative value. The exponent  $\alpha$  is directional, under the same wind directions, and decreases with the increase of wind speed.

6. The field measurement results of decay factors show that the winds are less coherent in comparison with that assumed in design, and the lateral component is more coherent than the longitudinal component and vertical component. The mean values of decay factors are  $C_{uu}=16.7$ ,  $C_{vv}=10.1$ , and  $C_{ww}=18.8$ , respectively.

7. The field measurement results have some difference to the recommended value. Therefore, a continuous and long-term field measurement should be carried out.

## References

- Dai, Y.M., Li, Z.N., Li, Q.S., Song, L.L., 2009. Wind loads on low-rise building: study on variation of near ground wind

profiles. *China Civil Engineering Journal*, **42**(3):42-48.

- Fu, J.Y., Li, Q.S., Wu, J.R., Xiao, Y.Q., Song, L.L., 2008. Field measurements of boundary layer wind characteristics and wind-induced responses of super-tall buildings. *Wind Engineering and Industrial Aerodynamics*, **96**(2008): 1332-1358. [doi:10.1016/j.jweia.2008.03.004]
- Hui, M.C.H., Larse, A., Xiang, H.F., 2009a. Wind turbulence characteristics study at the Stonecutters Bridge site: Part I-Mean wind and turbulence intensities. *Wind Engineering and Industrial Aerodynamics*, **97**(2009):22-36. [doi:10.1016/j.jweia.2008.11.002]
- Hui, M.C.H., Larse, A., Xiang, H.F., 2009b. Wind turbulence characteristics study at the Stonecutters Bridge site: Part II: wind power spectra, integral length scales and coherences. *Wind Engineering and Industrial Aerodynamics*, **97**(2009):48-59. [doi:10.1016/j.jweia.2008.11.003]
- Li, Q.S., Xiao, Y.Q., Fu, J.Y., Li, Z.N., 2007. Full-scale measurements of wind effects on the Jin Mao building. *Wind Engineering and Industrial Aerodynamics*, **95**(2007): 445-466. [doi:10.1016/j.jweia.2006.09.002]
- Li, Y.C., Wu, J.G., Xie, Z.Q., Jiao, S.M., Liu, C., 2008. Turbulent characteristic parameter of different strong wind sample. *Applied Meteorological Science*, **34**(19):28-34.
- Miyata, T., Yamada, H., Atsuchi, H.K., Itagawa, M.K., 2002. Full-scale measurement of Akashi-Kaikyo Bridge during typhoon. *Wind Engineering and Industrial Aerodynamics*, **90**(2002):1517-1527. [doi:10.1016/S0167-6105(02)00267-2]
- Pang, J.B., 2006. Field Investigation and Wind Tunnel Simulation of Strong Wind Characteristics in Coastal and Mountainous Regions. PhD Thesis, School of Civil Engineering, Tongji University, Shanghai, China (in Chinese).
- Solari, G., Piccardo, G., 2001. Probabilistic 3-D turbulence modeling for gust buffeting of structures. *Probabilistic Engineering Mechanics*, **16**(2001):73-86. [doi:10.1016/S0266-8920(00)00010-2]
- Tieleman, H.W., 1983. On the Wind Structure Near the Surface at a Mid-Atlantic Coastal Site. Proceedings of the 4th US National Conference on Wind Engineering Research Seattle, p.89-100.
- Toriumi, R., Katsuchi, H., Furuya, N., 2000. A study on spatial correlation of natural wind. *Wind Engineering and Industrial Aerodynamics*, **87**(2000):203-216.